Breaking through the Mermin-Wagner limit in 2D van der Waals magnets

Elton Santos (esantos@ed.ac.uk)
University of Edinburgh https://orcid.org/0000-0001-6065-5787
Sarah Jenkins
University of York
Levente Rózsa
University of Konstanz https://orcid.org/0000-0001-9456-5755
Unai Atxitia
Dahlem Center for Complex Quantum Systems and Fachbereich Physik, Freie Universitat Berlin
Richard Evans
University of York https://orcid.org/0000-0002-2378-8203
Konstantin Novoselov
National University Singapore https://orcid.org/0000-0003-4972-5371

Article

Keywords:

Posted Date: July 6th, 2022

DOI: https://doi.org/10.21203/rs.3.rs-1637788/v1

Additional Declarations: There is **NO** Competing Interest.

Version of Record: A version of this preprint was published at Nature Communications on November 14th, 2022. See the published version at https://doi.org/10.1038/s41467-022-34389-0.

Breaking through the Mermin-Wagner limit in 2D van der Waals magnets

Sarah Jenkins[1,2,3], Levente Rózsa[4], Unai Atxitia[5], Richard F. L. Evans[1], Kostya S. Novoselov[6], Elton J. G. Santos[7,8†]

[1]*Department of Physics, University of York, York, YO10 5DD, UK*

[2]*TWIST Group, Institut für Physik, Johannes Gutenberg Universität, 55128 Mainz, Germany*

[3]*TWIST Group, Institut für Physik, Universität Duisburg-Essen, Campus Duisburg, 47057 Duisburg, Germany*

[4]*Fachbereich Physik, Universität Konstanz, D-78457 Konstanz, Germany*

[5]*Dahlem Center for Complex Quantum Systems and Fachbereich Physik, Freie Universität Berlin, 14195 Berlin, Germany*

[6]*Institute for Functional Intelligent Materials, National University of Singapore, 117544, Singapore*

[7]*Institute for Condensed Matter Physics and Complex Systems, School of Physics and Astronomy, The University of Edinburgh, EH9 3FD, United Kingdom*

[8]*Higgs Centre for Theoretical Physics, The University of Edinburgh, EH9 3FD, United Kingdom*

[†]*Corresponding author: esantos@ed.ac.uk*

The Mermin-Wagner theorem [1] states that long-range magnetic order does not exist in one- or two-dimensional (2D) isotropic magnets with short-ranged interactions. The theorem has been a milestone on magnetism and has been driving the research of recently discovered 2D

van der Waals (vdW) magnetic materials[2,3] from fundamentals up to potential applications[4]. In such systems, the existence of magnetic ordering is typically attributed to the presence of a significant magnetic anisotropy, which is known to introduce a spin-wave gap and circumvent the core assumption of the theorem[1,5,6]. Here we show that in finite-size 2D vdW magnets typically found in lab setups (*e.g.,* within millimetres), short-range interactions can be large enough to allow the stabilisation of magnetic order at finite temperatures without any magnetic anisotropy for practical implementations. We demonstrate that magnetic ordering can be created in flakes of 2D materials independent of the lattice symmetry due to the intrinsic nature of the spin exchange interactions and finite-size effects in two-dimensions. Surprisingly we find that the crossover temperature, where the intrinsic magnetisation changes from superparamagnetic to a completely disordered paramagnetic regime, is weakly dependent on the system length, requiring giant sizes (*e.g.,* of the order of the observable universe $\sim 10^{26}$ m) in order to observe the vanishing of the magnetic order at cryogenic temperatures as expected from the Mermin-Wagner theorem. Our findings indicate exchange interactions as the main driving force behind the stabilisation of short-range order in 2D magnetism and broaden the horizons of possibilities for exploration of compounds with low anisotropy at an atomically thin level.

Introduction

The demand for computational power is increasing exponentially, following the amount of data generated across different devices, applications and cloud platforms[7,8]. To keep up with this trend,

smaller and increasingly energy-efficient devices must be developed which require the study of compounds not yet explored in data-storage technologies. The discovery of magnetically stable 2D vdW materials could allow for the development of spintronic devices with unprecedented power efficiency and computing capabilities that would in principle address some of these challenges[4]. Indeed, the magnetic stability of vdW layers has been one of the central limitations for finding suitable candidates, given that strong thermal fluctuations are able to rule out any magnetism. As it was initially pointed out by Hohenberg[6] for a superfluid or a superconductor, and extended by Mermin and Wagner[1] for spins on a lattice, long-range order should be suppressed at finite temperatures in the 2D regime, when only short-range isotropic interactions exist. Importantly, the theorem only excludes long-range magnetic order at finite temperature in the thermodynamic limit[1], *i.e.,* for infinite system sizes. However, the common understanding is that the theorem also excludes the alignment of spins in samples studied experimentally which are a few micrometers in size[9,10], suggesting that such systems are indistinguishable from infinite.

The long-range order characterising infinite systems only becomes distinguishable from short-range order describing the local alignment of the spins if the system size exceeds the correlation length at a given temperature[11]. Previous numerical studies and the scaling analysis of 2D Heisenberg magnets[12–15] have established that although only short-range order is observable at finite temperature, the spin correlation length can be larger than the system size below some finite crossover temperatures. An intriguing question on this long-range limit is how can we understand real-life materials, which routinely have a finite size L (Fig. 1**a**), in light of the Mermin-Wagner theorem. It is known that thermal fluctuations will affect the emergence of a spontaneous mag-

netisation at low dimensionality. Nevertheless, it is unclear which kind of spin ordering can be foreseen in thin vdW layered compounds when finite-size effects and exchange interactions play together. With recent advances in computational power and parallelisation scalability, it is possible to directly model magnetic ordering processes and dynamics of 2D materials on the micrometre length-scale accessible experimentally. Here, we demonstrate that short-range order can exist in systems with no anisotropy even down to the 2D limit using computer-intensive atomistic simulations and analytical models.

Results

We start by defining the magnetization in our systems as:

$$\mathbf{m} = \frac{1}{N}\sum_i \mathbf{S}_i, \tag{1}$$

where $\mathbf{S}_i$ denotes the classical spin unit vector at lattice site i and N is the number of sites. In the absence of external magnetic fields, the expectation value of the magnetization $\langle \mathbf{m} \rangle$ vanishes in any finite-size system due to time-reversal invariance. Yet, 3D systems of only a few nanometres in size that are far from infinite have been studied for decades and exhibit a clear crossover from a magnetically ordered to a paramagnetic phase [16,17]. The Mermin-Wagner theorem establishes that $\langle \mathbf{m} \rangle$ must also be zero in infinite 2D systems with short-ranged isotropic interactions. However, for practical implementations it is relevant to unveil whether the average magnetisation vanishes because the spins are completely disordered at any point in time, or if they are still aligned on short distances but the overall direction of the magnetisation $\mathbf{m}$ strongly suffers time-dependent

variation. Short-range order may be characterised by the intrinsic magnetisation[18]:

$$\langle|\mathbf{m}|\rangle = \left\langle \sqrt{\left(\frac{1}{N}\sum_i \mathbf{S}_i\right)^2} \right\rangle, \tag{2}$$

which is always positive by definition. The intrinsic magnetisation is close to 1 ($\langle|\mathbf{m}|\rangle = 1$) in the short-range-ordered regime and converges to zero when the spins become completely disordered[9,19,20].

For simplicity we first consider a 2D honeycomb lattice (Fig. 1**a**) to model the magnetic ordering process for a large flake of 1000×1000 nm^2. Such a symmetry is very common in several vdW materials holding magnetic properties and interfaces[4], such as $Cr_2Ge_2Te_6$ (CGT) or CrI_3 in which 2D magnetic ordering was first discovered[2,3]. The system consists of 8 million atoms with nearest-neighbor Heisenberg exchange interactions ($J_{ij}/k_B = 70.8$ K) and no magnetic anisotropy (K) using highly accurate Monte Carlo simulations (see Supplementary Sections 1-2 for details). The magnitude of J_{ij}/k_B is within the same range as those observed for CGT (with a critical temperature of 66 K)[2] where a negligible magnetic anisotropy (< 1 μeV) was observed for thin layers but a stable magnetic signal was still measured at finite temperatures ($\sim$4.7 K)[2]. Indeed, as we show below, thermal fluctuations do not destroy the short-range magnetic order but rather induce the formation of strongly correlated spins at large spatial scale. We use an isotropic Heisenberg spin Hamiltonian $\mathscr{H} = -\sum_{i<j} J_{ij}\mathbf{S}_i \cdot \mathbf{S}_j$ as stated in the Mermin-Wagner theorem[1]. We begin by assessing the existence of any magnetic order at non-zero temperatures by equilibrating the system for 39×10^6 Monte Carlo steps using a uniform sampling[21] to avoid any potential bias before a final averaging at thermal equilibrium for a further 10^6 Monte Carlo

steps. Strikingly, a crossover between the low-temperature short-range-ordered regime and the completely disordered state ($\langle|\mathbf{m}|\rangle \approx 0$) is observed at nonzero temperatures (Fig. 1**b**) and zero magnetic anisotropy ($K = 0$). To estimate the crossover temperature (T_x), the simulation data was fitted by the Curie-Bloch equation in the classical limit[9]:

$$\langle|\mathbf{m}|\rangle(T) = \left(1 - \frac{T}{T_x}\right)^{\beta}, \tag{3}$$

where T is the temperature and β is the crossover magnetization exponent. From the fitting one obtains $T_x = 23.342 \pm 0.237$ K ($\beta = 0.54 \pm 0.020$), which is about one third of the mean-field (MF) critical temperature $T_c^{\mathrm{MF}} = zJ_{ij}/(3k_B) = 70.8$ K (where $z = 3$ is the number of nearest neighbours) even for this considerable system size. The simulations were then repeated including magnetic anisotropy ($K = 1 \times 10^{-24}$ J/atom) which resulted in a slight increase in the crossover temperature ($T_x = 26.543 \pm 0.320$ K, $\beta = 0.427 \pm 0.021$) (Fig. 1**b**). We observed that this difference in T_x between isotropic and anisotropic cases becomes negligible as the flake size is reduced (100×100 nm^2) with minor variations of the curvature of the magnetisation versus temperature (Supplementary Section 3 and Supplementary Figure 1). We also checked that different Monte Carlo sampling algorithms (*i.e.,* adaptive) and starting spin configurations (*i.e.,* ordered, disordered) do not modify the overall conclusions (Supplementary Section 4 and Supplementary Figure 2). Taking dipolar interactions into account only has a minor effect on the intrinsic magnetization curve (Supplementary Figure 3). Although the magnetocrystalline anisotropy K or the dipolar interactions circumvent the Mermin-Wagner theorem and lead to a finite critical temperature, this indicates that systems up to lateral sizes of 1 μm are not suitable for observing the critical behaviour. Instead the crossover in the short-range order defined by the isotropic interactions dominates in this regime, regardless of

whether the anisotropy is present or absent. Previous studies on finite magnetic clusters on metallic surfaces[22,23] suggested that anisotropy is not the key factor in the stabilisation of magnetic properties at low dimensionality and finite temperatures, but rather it determines the orientation of the magnetisation.

Even though short-range interactions can stabilise short-range magnetic order in 2D vdW magnetic materials, this does not necessarily imply that the direction or the magnitude of the magnetisation is stable over time. As thermally activated magnetisation dynamics may potentially change spin directions[24], it is important to clarify whether angular variations of the spins are present. Hence we compute the time evolution of the magnetisation along different directions (x, y, z) and its angular dependence (Fig. 1**c,d**) through the numerical solution of the Landau-Lifshitz-Gilbert equation (see Methods for details). Over the whole simulation (40 ns), all components of the magnetisation assume approximately constant values which deviates by $\pm 5^{\circ}$ from the mean direction θ_{av}. Similar analyses undertaken for different flake sizes ($L \times L$, $L = 50$, 100, 500 nm) show that the spin direction is very stable at each temperature considered (2.5 K, 10 K, 20 K, 30 K, 40 K) and follows a Boltzmann distribution (Supplementary Section 5 and Supplementary Figure 4). These results show that the magnetisation in a 2D isotropic magnet is not only stable in magnitude but its direction only negligibly varies over time.

An outstanding question raised by the modelling of the 2D finite flakes is whether other kind of common lattice symmetries (*i.e.,* hexagonal, square), lower dimensions (*i.e.,* 1D) and different sizes may follow similar behaviour to that found in the honeycomb lattice. Figure 2 shows that

the effect is universal regardless of the details of the lattice or the dimension considered. We find persistent magnetic order for $T > 0$ K at zero magnetic anisotropy for the cases considered. There is a consistent reduction in the crossover temperature as a function of the system size $L \to \infty$ in agreement with the general trend of the temperature dependence of the correlation length discussed above (Fig. 2**a-c**). The 1D model (atomic chain) displays a similar trend (Fig. 2**d**) although the variation of $\langle|\mathbf{m}|\rangle$ with T is different due to the lower dimensionality.

To give an analytical description of these effects, we use the anisotropic spherical model (ASM) for the calculation of the finite-size effects on the intrinsic magnetization[18,25,26] (see Supplementary Section 7 for details). The ASM takes into account Goldstone modes in the system and self-consistently generates a gap in the correlation functions which avoids infrared divergences responsible for the absence of long-range order for isotropic systems in dimensions $d \leq 2$ as $L \to \infty$ as per the Mermin-Wagner theorem. We applied the formalism to 1D and 2D systems for the isotropic Heisenberg Hamiltonian in the absence of an external magnetic field[18]. The results of our analytical calculations are shown as shaded regions in Fig. 2 (see Supplementary Section 7 for the definition of the regions). At low temperatures both limits agree well with our Monte Carlo calculations within the statistical noise and clearly show the existence of a finite intrinsic magnetisation at non-zero temperature for finite size. At higher temperatures there is a systematic difference between the degree of magnetic ordering between the simulations and the analytical calculations due to the ASM only becoming exact in the limit of infinitely many spin components. The large number of Monte Carlo steps and strict convergence criteria to the same thermodynamic equilibrium for ordered and disordered starting states (see Supplementary Section 4) rule out critical slowing

down[27] as a source of difference between the analytical calculations and the simulations.

One may also argue in terms of the correlation length ξ which is comparable to the system size at the crossover temperature. It has been demonstrated[13] that $\xi \propto \exp(cJ/T)$, where c is a constant, meaning that the inverse crossover temperature T_x^{-1} only logarithmically increases with the system size. Although our simulations are at the limit of the capabilities of current supercomputer features, this effect is expected to persist for larger sizes of $2-10$ μm. These values represent typical sizes of continuous 2D microflakes in experiments, and much larger than the ideal nanoscale devices likely to be used in future 2D spintronic applications. Fitting a scaling function to the crossover temperatures for different lattice symmetries (Fig. 2), we can plot the scaling of the crossover temperature with size (Fig. 3**a**) which can then be extrapolated to larger scales. The crossover temperature is still approximately 30 K for $2-10$ μm flakes (Fig.3**b**). The graph can be extrapolated to show that only at the $10^{15}-10^{25}$ m range does the crossover temperature become lower than $\sim$1 K. To put these numbers in perspective to physical systems, these length scales lie between the distance of the Earth to the Sun and the diameter of the observable universe. Therefore, the often asserted notion[4] that experimental 2D magnetic samples can be classified as infinite and therefore display no net magnetic order at nonzero temperatures, as expected from the Mermin-Wagner theorem, is not applicable.

The significance of the crossover temperature T_x in relation to the Curie temperature T_C is particularly important when discussing the nature of the magnetic ordering in 2D magnets at zero anisotropy for $T > 0$ K. We investigate this behaviour through colour maps of the spin ordering

after 40 million Monte Carlo steps comparing different system sizes and temperatures (Fig. 4). At very low temperatures $T = 2.5$ K, where there is a high degree of order, the spin directions are highly correlated, as indicated by a mostly uniform colouring. Although the temperatures are near zero, the system is superparamagnetic indicating that over time the magnetization direction fluctuates, and the effect is most apparent for the smallest sizes where the average direction has moved significantly from the initial direction $\mathbf{S}||z$. At higher temperatures the deviation of the spin directions within the sample increases as indicated by the more varied colouring. To quantitatively assess the spin deviations we plot the statistical distribution of angle between the spin direction and the mean direction for different temperatures for each size (Supplementary Figure 4). For an isotropic distribution on the unit sphere there is a $\sin(\theta)$ weighting which is seen at the highest temperature for all system sizes. For lower temperatures where the spin directions are more correlated, the distribution is biased towards lower angles. Qualitatively there is little difference in the spin distributions for the different samples. At $T = 20$ K there is however a systematic trend in the peak angle increasing from $\theta = 40^\circ$ for the 50×50 nm^2 flake (Supplementary Figure 4**a**) to around $\theta = 60^\circ$ at 1000×1000 nm^2 (Supplementary Figure 4**d**) indicating an increased level of disorder averaged over the whole sample. This effect is straightforwardly explained by the size dependence of spin-spin correlations. At small sizes the spins are strongly exchange coupled, preventing large local deviations of the spin directions. At longer length scales available for the larger systems, the variations in the magnetisation direction are also larger. Surprisingly, our calculations reveal that this effect is weak: even for very large flakes of a micrometre in size, only a small increase can be observed in the position of the peak in the angle distribution at a fixed temperature.

Above the crossover temperature the spin-spin correlation length becomes very small compared to the system size with rapid local changes in the magnetisation direction, indicative of a completely disordered paramagnetic state. Our analysis reveals that the spins in finite-sized 2D isotropic magnets are strongly aligned due to short-range order at non-zero temperatures and up to the crossover temperature.

Discussion

Mathematically a phase transition is defined as a non-analytic change in the state variable for the system, such as the particle density or the magnetization in the case of spin systems. For any finite system the state variable is continuous by definition due to a finite number of particles, forming a continuous path of intermediate states between two distinct physical phases[28]. The same is true for a magnetic system, forming a continuous path between an ordered and a paramagnetic state. A priori then, it is impossible to have a true phase transition for any finite magnetic samples which are routinely implemented in device platforms. Yet, nanoscale magnets that are far from infinite have been studied for decades and exhibit a clear crossover from magnetically ordered to paramagnetic phases, occurring for systems only a few nanometres in size[16,17]. The crossover temperature in a finite-size system hence can be described as an inflection point in M(T). The precise definition of a phase transition is significant when considering the main conclusions of Mermin and Wagner[1], which explicitly only apply in the case of an infinite system. As our results clearly show, sample sizes measured experimentally are not classifiable as infinite and therefore not subject to the Mermin-Wagner theorem. It is noteworthy that 3D compounds have weak dependence of their

critical temperature on the magnetic anisotropy[29]. Similar analysis performed for a finite 3D honeycomb bulk system (Supplementary Figure 6**a-b**) show that the inclusion of anisotropy barely change the results for Tc. This suggests that magnetism is an exchange-driven effect in both two and three dimensions.

On the practical side, heterostructures with conventional metallic magnetic materials could establish preferential directions of the magnetization through anisotropic exchange and dipolar couplings. However, it is important to point out that the short-range order is enforced by the isotropic exchange couplings and even a low anisotropy may suffice for stabilizing the direction of the magnetization at the vdW layers, *i.e.,* from underlying magnetic substrates. We can imagine micrometre-sized samples where all spins are still correlated at finite temperatures so it could represent a single bit. However, for miniaturization purposes multiple nanometre-sized bits are required on the same sample in order to be implemented in recording media. This is typically achieved by magnetic domains, but there are no domains in an isotropic model since the domain wall width is infinite. However, if vdW layers can be grown with grain boundaries, like in 2D mosaics[30], which are large enough that each grain area would have an uniform magnetisation, then a magnetic monolayer would have as many bits as available on the material surface. The underlying substrate hence would set the magnetisation direction for further implementations. This spin-interface engineering would be a considerable step towards on-demand magnetic properties at the atomic level given the flexibility on the orientation of the magnetic moments without a predefined direction at the layer. While the anisotropy circumvents the Mermin-Wagner theorem and causes the critical temperature T_c to be nonzero in infinitely large systems, in finite samples

the short-range order persists up to much higher temperatures ($T_x > T_c$) since T_x is proportional to the isotropic exchange rather than the anisotropy[31,32].

In conclusion, we presented large-scale spin dynamic simulations and analytical calculations of the temperature dependence of the intrinsic magnetization in 2D magnetic materials described by an isotropic Heisenberg model. We found that short-range magnetic order at non-zero temperature is a robust feature of isotropic 2D magnets even at experimentally accessible length and time scales. Our data show that the often asserted Mermin-Wagner limit[1] does not apply to 2D materials on real laboratory sample sizes . Since the spins are aligned due to the exchange interactions already in the isotropic model, the direction of the magnetization may be stabilized by geometrical factors or finite-size effects. These findings open up possibilities for a wider range of 2D magnetic materials in device applications than previously envisioned. Furthermore, the limited applicability of the analytical Mermin-Wagner theorem opens similar possibilities in other fields such as superconductivity and liquid crystal systems[33], where the relevant length scale of correlations is known to be much greater than that required for experimental measurements and applications. Our results suggest that if the magnetic anisotropy can be controlled to a certain degree[34] until it completely vanishes, new effects of strongly correlated spins or more unusual disordered states may be observed.

Methods

We used atomistic simulations methods[9,35] to compute the magnetic properties of 2D magnetic materials. The energy of our system is calculated using the spin Hamiltonian:

$$\mathscr{H} = -\sum_{i<j} J_{ij}\mathbf{S}_i \cdot \mathbf{S}_j - K\sum_i (S_i^z)^2, \tag{4}$$

where $\mathbf{S}_{i,j}$ are unit vectors describing the local spin directions on magnetic sites i, j, and J_{ij} is the exchange constant between spins.An easy-axis magnetocrystalline anisotropy constant K can be included as well, with negligible modifications of the results as described in the text. Simulations were run for system sizes of 50 nm, 100 nm, 500 nm and 1000 nm laterally along the x and y directions and 1 atomic layer thick along the z direction. For the honeycomb lattice, the simulations were initialized in either a perfectly ordered state aligned along the z direction or a random state corresponding to infinite temperature. For these simulations the final $\langle|\mathbf{m}|\rangle(T)$ curves were identical to each other. However, at low temperatures it took ten times as many steps to reach the final equilibrium state from the random state, so for the remaining structures only simulations starting from the ordered states were run. The systems were integrated using a Monte Carlo integrator using a uniform sampling algorithm[36] to remove any bias introduced from more advanced algorithms[21]. To investigate the temperature dependence, the simulation temperature was varied from 0 to 90 K in 2.5 K steps. 40×10^6 Monte Carlo steps were run for each temperature step. This was split into 39×10^6 equilibration steps and then 10^6 time steps from which the statistics were calculated. The Monte Carlo simulations use a pseudo-random number sequence generated by the Mersenne Twister algorithm[37] due to its high quality, avoiding correlations in the generated

255 random numbers and with an exceptionally long period of $2^{19937}-1 \sim 10^{6000}$. The parallel im-
256 plementation generates different random seeds on each processor to ensure no correlation between
257 the generated random numbers.

The time-dependent simulations in Fig. 1**c,d** were performed by solving the stochastic Landau-Lifshitz-Gilbert equation:

$$\frac{\partial \mathbf{S}_i}{\partial t} = -\frac{\gamma_e}{1+\lambda^2}\left[\mathbf{S}_i \times \mathbf{B}_{\text{eff}} + \lambda \mathbf{S}_i \left(\mathbf{S}_i \times \mathbf{B}_{\text{eff}}\right)\right], \tag{5}$$

which models the interaction of an atomic spin moment $\mathbf{S}_i$ with an effective magnetic field $\mathbf{B}_{\text{eff}} = -\partial\mathscr{H}/\partial\mathbf{S}_i$. The effective field causes the atomic moments to precess around the field, where the frequency of precession is determined by the gyromagnetic ratio of an electron ($\gamma_e = 1.76 \times 10^{11}$ rad $\text{s}^{-1}\text{T}^{-1}$) and $\lambda = 1$ is the damping constant. The effect of temperature is taken into account using Langevin dynamics[38], where the thermal fluctuations are represented by a Gaussian white noise term. At each time step the instantaneous thermal field acting on each spin is given by

$$\mathbf{B}^i_{\text{th}} = \sqrt{\frac{2\lambda k_B T}{\gamma \mu_s \Delta t}}\mathbf{\Gamma}(t) \tag{6}$$

258 where k_{B} is the Boltzmann constant, T is the system temperature and $\mathbf{\Gamma}(t)$ is a vector of standard
259 (mean 0, variance 1) normal variables which are independent in components and in time. The
260 thermal field is added to the effective field in order to simulate a heat bath. The system was
261 integrated using a Heun numerical scheme[36].

Acknowledgments

We thank David Mermin, Mikhail Katsnelson, and Bertrand Halperin for valuable discussions. E.J.G.S. acknowledges computational resources through CIRRUS Tier-2 HPC Service (ec131 Cirrus Project) at EPCC (http://www.cirrus.ac.uk) funded by the University of Edinburgh and EPSRC (EP/P020267/1); ARCHER UK National Supercomputing Service (http://www.archer.ac.uk) *via* Project d429. EJGS acknowledges the Spanish Ministry of Science's grant program "Europa-Excelencia" under grant number EUR2020-112238, the EPSRC Early Career Fellowship (EP/T021578/1), and the University of Edinburgh for funding support.

Supplementary Materials

Supplementary Sections 1-7, Supplementary Figures 1-5, and Supplementary References.

Data Availability

The data that support the findings of this study are available within the paper and its Supplementary Information.

Competing interests

The Authors declare no conflict of interests.

Author Contributions

EJGS conceived the idea and supervised the project. SJ performed the atomistic simulations with inputs from EJGS and RFLE. LR and UA developed the semi-analytical model and undertook the numerical simulations. EJGS wrote the paper with a draft initially prepared by SJ and RFLE and also with inputs from KSN, UA and LR. All authors contributed to this work, read the manuscript, discussed the results, and agreed on the included contents.

References

1. Mermin, N. D. & Wagner, H. Absence of Ferromagnetism or Antiferromagnetism in One- or Two-Dimensional Isotropic Heisenberg Models. *Physical Review Letters* **17**, 1133–1136 (1966). URL https://link.aps.org/doi/10.1103/PhysRevLett.17.1133.

2. Gong, C. *et al.* Discovery of intrinsic ferromagnetism in two-dimensional van der waals crystals. *Nature* **546**, 265–269 (2017). URL http://www.nature.com/articles/nature22060.

3. Huang, B. *et al.* Layer-dependent ferromagnetism in a van der Waals crystal down to the monolayer limit. *Nature* **546**, 270–273 (2017). URL https://doi.org/10.1038/nature22391.

4. Wang, Q. H. *et al.* The magnetic genome of two-dimensional van der waals materials. *ACS Nano* (2022).

5. Bogolyubov, N. N. *Quasi-Averages in Problems of Statistical Mechanics*, chap. Chapter 2, 21–99 (2014). URL https://www.worldscientific.com/doi/abs/10.1142/9789814612524_0002. https://www.worldscientific.com/doi/pdf/10.1142/9789814612524_0002.

6. Hohenberg, P. C. Existence of long-range order in 1 and 2 dimensions. *Phys. Rev.* **158**, 383–386 (1967).

7. Dieny, B. *et al.* Opportunities and challenges for spintronics in the microelectronics industry. *Nature Electronics* **3**, 446–459 (2020).

8. Sander, D. *et al.* The 2017 magnetism roadmap. *Journal of Physics D: Applied Physics* **50**, 363001 (2017).

9. Wahab, D. A. *et al.* Quantum rescaling, domain metastability, and hybrid domain-walls in 2d CrI_3 magnets. *Adv. Mater.* **33**, 2004138 (2021). URL https://doi.org/10.1002/adma.202004138. https://onlinelibrary.wiley.com/doi/pdf/10.1002/adma.202004138.

10. Kim, M. *et al.* Micromagnetometry of two-dimensional ferromagnets. *Nature Electronics* **2**, 457–463 (2019).

11. Halperin, B. I. On the hohenberg–mermin–wagner theorem and its limitations. *Journal of Statistical Physics* **175**, 521–529 (2019).

12. Stanley, H. E. & Kaplan, T. A. Possibility of a Phase Transition for the Two-Dimensional Heisenberg Model. *Physical Review Letters* **17**, 913–915 (1966). URL https://link.aps.org/doi/10.1103/PhysRevLett.17.913.

13. Shenker, S. H. & Tobochnik, J. Monte Carlo renormalization-group analysis of the classical Heisenberg model in two dimensions. *Physical Review B* **22**, 4462–4472 (1980). URL https://link.aps.org/doi/10.1103/PhysRevB.22.4462.

14. Blöte, H. W. J., Guo, W. & Hilhorst, H. J. Phase transition in a two-dimensional Heisenberg model. *Phys. Rev. Lett.* **88**, 047203 (2002). URL https://link.aps.org/doi/10.1103/PhysRevLett.88.047203.

15. Tomita, Y. Finite-size scaling analysis of pseudocritical region in two-dimensional continuous-spin systems. *Phys. Rev. E* **90**, 032109 (2014). URL https://link.aps.org/doi/10.1103/PhysRevE.90.032109.

16. Roduner, E. Size matters: why nanomaterials are different. *Chem. Soc. Rev.* **35**, 583–592 (2006).

17. Singh, R. Unexpected magnetism in nanomaterials. *Journal of Magnetism and Magnetic Materials* **346**, 58–73 (2013).

18. Kachkachi, H. & Garanin, D. A. Boundary and finite-size effects in small magnetic systems. *Physica A: Statistical Mechanics and its Applications* **300**, 487–504 (2001). URL https://www.sciencedirect.com/science/article/pii/S0378437101003612.

19. Sun, Q.-C. *et al.* Magnetic domains and domain wall pinning in atomically thin crbr3 revealed by nanoscale imaging. *Nature Communications* **12**, 1989 (2021).

20. Abdul-Wahab, D. *et al.* Domain wall dynamics in two-dimensional van der Waals ferromagnets. *Appl. Phys. Rev.* **8**, 041411 (2021).

21. Alzate-Cardona, J. D., Sabogal-Suárez, D., Evans, R. F. L. & Restrepo-Parra, E. Optimal phase space sampling for Monte Carlo simulations of Heisenberg spin systems. *Journal of Physics: Condensed Matter* **31**, 095802 (2019). URL https://doi.org/10.1088%2F1361-648x%2Faaf852.

22. Minár, J., Bornemann, S., Šipr, O., Polesya, S. & Ebert, H. Magnetic properties of co clusters deposited on pt(111). *Applied Physics A* **82**, 139–144 (2006).

23. Šipr, O. *et al.* Magnetic moments, exchange coupling, and crossover temperatures of co clusters on pt(111) and au(111). *Journal of Physics: Condensed Matter* **19**, 096203 (2007).

24. Brown, W. F. Thermal fluctuations of a single-domain particle. *Phys. Rev.* **130**, 1677–1686 (1963). URL https://link.aps.org/doi/10.1103/PhysRev.130.1677.

25. Garanin, D. A. Spherical model for anisotropic ferromagnetic films. *Journal of Physics A: Mathematical and General* **29**, L257–L262 (1996). URL http://dx.doi.org/10.1088/0305-4470/29/10/006.

26. Garanin, D. A. Ordering in magnetic films with surface anisotropy. *Journal of Physics A: Mathematical and General* **32**, 4323–4342 (1999). URL http://dx.doi.org/10.1088/0305-4470/32/24/301.

27. Nightingale, M. P. & Blöte, H. W. J. Dynamic exponent of the two-dimensional Ising model and Monte Carlo computation of the subdominant eigenvalue of the stochastic matrix. *Phys. Rev. Lett.* **76**, 4548–4551 (1996). URL https://link.aps.org/doi/10.1103/PhysRevLett.76.4548.

28. Stanley, H. *Introduction to Phase Transitions and Critical Phenomena*. International series of monographs on physics (Oxford University Press, 1971). URL https://books.google.co.uk/books?id=4K_vAAAAMAAJ.

29. Coey, J. M. D. *Magnetism and Magnetic Materials* (Cambridge University Press, Cambridge, 2010).

30. Yao, W., Wu, B. & Liu, Y. Growth and grain boundaries in 2d materials. *ACS Nano* **14**, 9320–9346 (2020).

31. Irkhin, V. Y., Katanin, A. A. & Katsnelson, M. I. Self-consistent spin-wave theory of layered heisenberg magnets. *Phys. Rev. B* **60**, 1082–1099 (1999). URL https://link.aps.org/doi/10.1103/PhysRevB.60.1082.

32. Grechnev, A., Irkhin, V. Y., Katsnelson, M. I. & Eriksson, O. Thermodynamics of a two-dimensional heisenberg ferromagnet with dipolar interaction. *Phys. Rev. B* **71**, 024427 (2005). URL https://link.aps.org/doi/10.1103/PhysRevB.71.024427.

33. Illing, B. *et al.* Mermin–Wagner fluctuations in 2d amorphous solids. *Proceedings of the National Academy of Sciences* **114**, 1856–1861 (2017). URL https://www.pnas.org/content/114/8/1856. https://www.pnas.org/content/114/8/1856.full.pdf.

34. Verzhbitskiy, I. A. *et al.* Controlling the magnetic anisotropy in $cr_2ge_2te_6$ by electrostatic gating. *Nat. Electron.* **3**, 460–465 (2020). URL http://www.nature.com/articles/s41928-020-0427-7.

35. Kartsev, A., Augustin, M., Evans, R. F. L., Novoselov, K. S. & Santos, E. J. G. Biquadratic exchange interactions in two-dimensional magnets. *npj Comput. Mater.* **6**, 150 (2020). URL https://doi.org/10.1038/s41524-020-00416-1.

36. Evans, R. F. *et al.* Atomistic spin model simulations of magnetic nanomaterials. *Journal of Physics Condensed Matter* **26** (2014).

379 37. Matsumoto, M. & Nishimura, T. Mersenne twister: a 623-dimensionally equidistributed uni-
380 form pseudo-random number generator. *ACM Trans. Model. Comput. Simul.* **8**, 3–30 (1998).

381 38. Brown, W. Thermal fluctuation of fine ferromagnetic particles. *IEEE Transactions on Mag-*
382 *netics* **15**, 1196–1208 (1979).

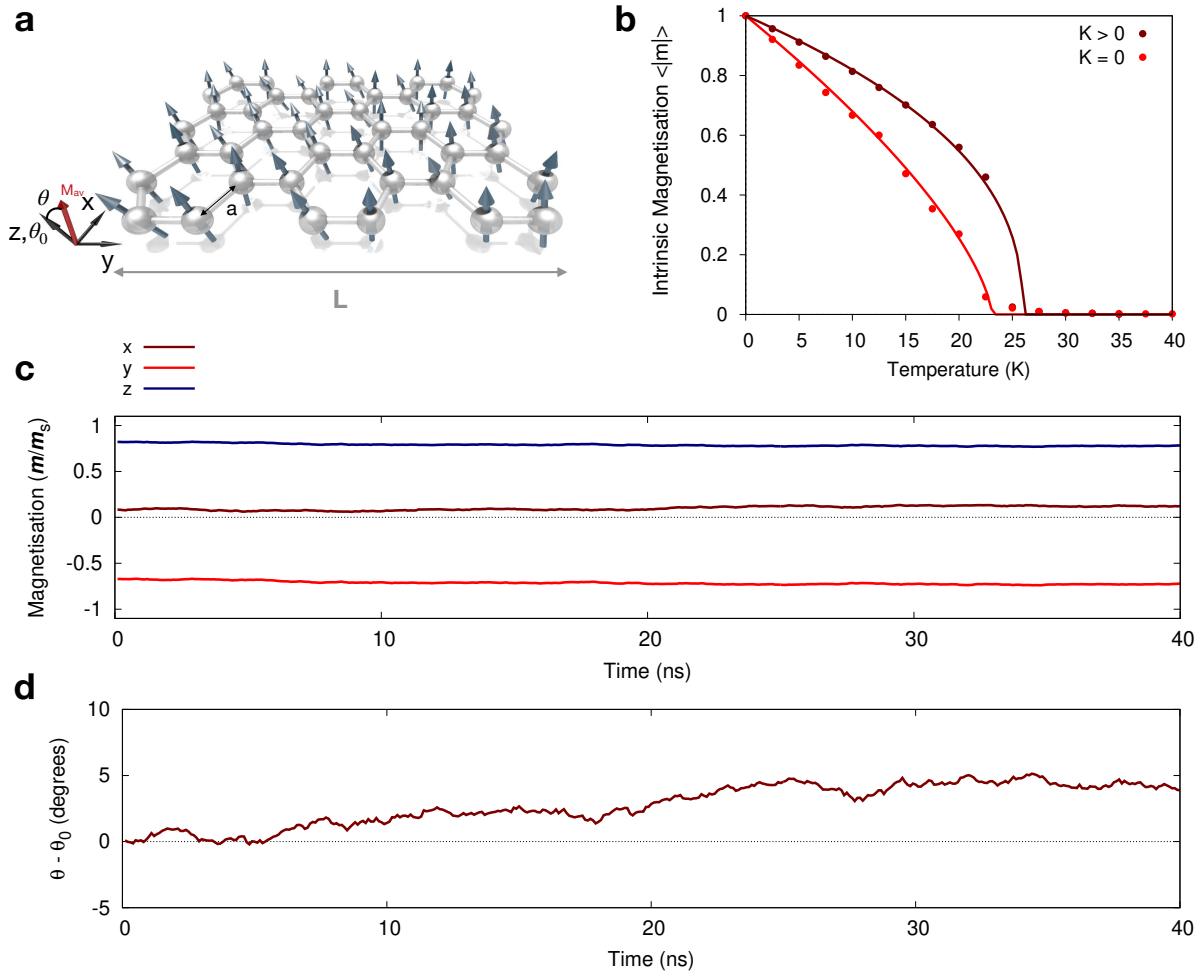

Figure 1: **Short-range magnetic ordering at finite temperatures in a 2D isotropic magnet. a,** Local view of the spin directions extracted from the atomistic simulations on a 2D honeycomb lattice. a is the atomic spacing ($a = 0.4$ nm), L is the length considered in the computations, and $\mathbf{M}_{av}$ is the averaged magnetisation vector. θ corresponds to the angle between $\mathbf{M}_{av}$ and the z-axis. $\theta_0 = 0$ denotes the initial configuration aligned with the z-axis. **b,** Temperature-dependent intrinsic magnetisation ($\langle|\mathbf{m}|\rangle$) with ($K = 1\times10^{-24}$ J/atom) and without ($K = 0$) anisotropy in a 1000×1000 nm^2 flake. Solid lines are the fit to Eq. (3). For $K = 0$, the fitting parameters are $\beta = 0.54\pm0.020$ and $T_x = 23.342\pm0.237$ K. For $K > 0$, $\beta = 0.427\pm0.021$ and $T_x = 26.543\pm0.320$ K. **c-d,** Temporal variation of the magnetisation (m/m_s) and angle $\theta - \theta_0$, respectively, at $T = 10$ K. All three spatial components (x, y, z) are considered in **c**. The dashed line in **d** shows the initial state in the simulations.

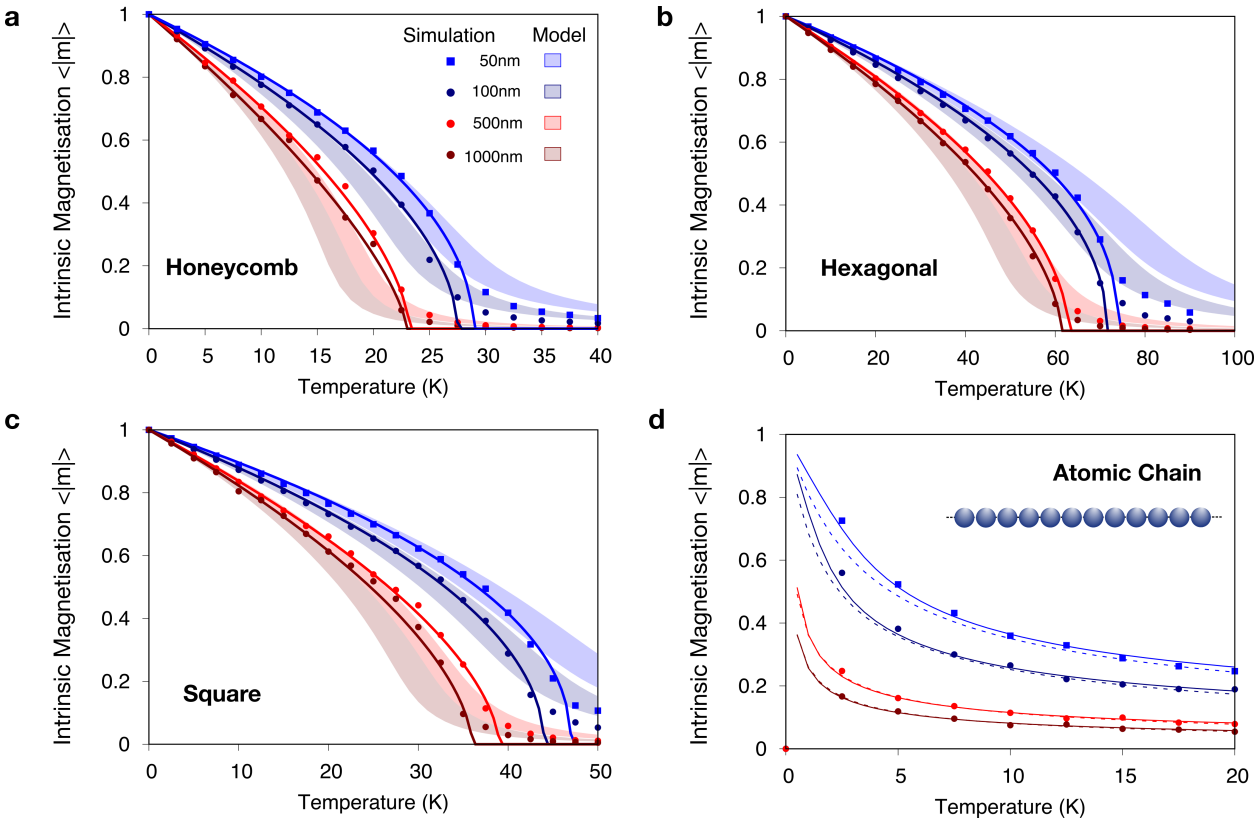

Figure 2: **Temperature- and size-dependent properties of isotropic 1D and 2D materials with different crystal structures. a-d** Comparative simulations of the temperature-dependent magnetisation for honeycomb, hexagonal, square lattices and an atomic chain (1D), respectively, for different system sizes. Points indicate the results of Monte Carlo simulations, the lines show fits to the Curie-Bloch Eq. (3) in the classical limit, and the shaded regions indicate the anisotropic spherical model calculations for different assumptions of the renormalisation factor for the Curie temperature arising from the mean-field approximation. See Supplementary Section 7 for details. The dashed and solid lines in **d** indicate the anisotropic spherical model calculations, and the exact solution, respectively. Both show a sound agreement with the atomistic simulations. The datasets in **a-c** clearly show the existence of short-range collinear magnetic order for all 2D lattices at the simulated sizes considered with nonzero crossover temperature. Zero magnetic anisotropy is included in all calculations.

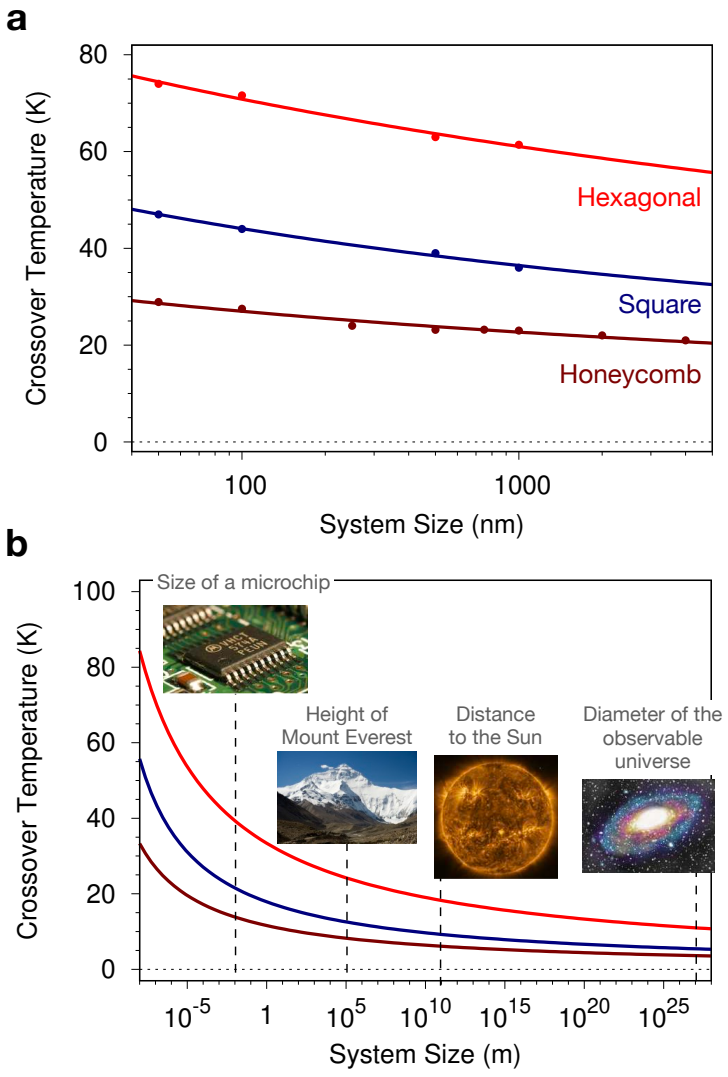

Figure 3: **Size scaling of the simulated crossover temperature for the different 2D lattices a,** Variation of the crossover temperature T_x with system size for different symmetries (Hexagonal, Square, Honeycomb) on a log-scale. The curves are a fit using $T_x = A/\log(L/B)$, where A and B are fitting constants and L is the system size. A and B are 327.28 K and 0.000542 nm, 484.96 K and 0.00166 nm and 1018.50 K and 5.7×10^{-5} nm for honeycomb, square and hexagonal lattices, respectively. **b,** Extrapolation of the exponential fits in **a** to larger sizes on all studied symmetries. The crossover temperature remains finite (>4 K) for systems as large as $\sim10^{25}$ m indicating no dependence of the magnetic anisotropy for stabilisation of magnetic ordering. Insets provide comparison with physical distances observed in different systems. Figures in **b** are adapted with permission under a Creative Commons CC BY license from Wiki Commons. Microchip: Integrated circuit on microchip by Jon Sullivan, 2006. Sun: inset is from ESA & NASA/Solar Orbiter/EUI team, 2022. Data processing by E. Kraaikamp. Everest: Mount Everest North Face as seen from the path to the base camp by Luca Galuzzi, 2006. Galaxy: artist view by Sarah Anthony, 2019.

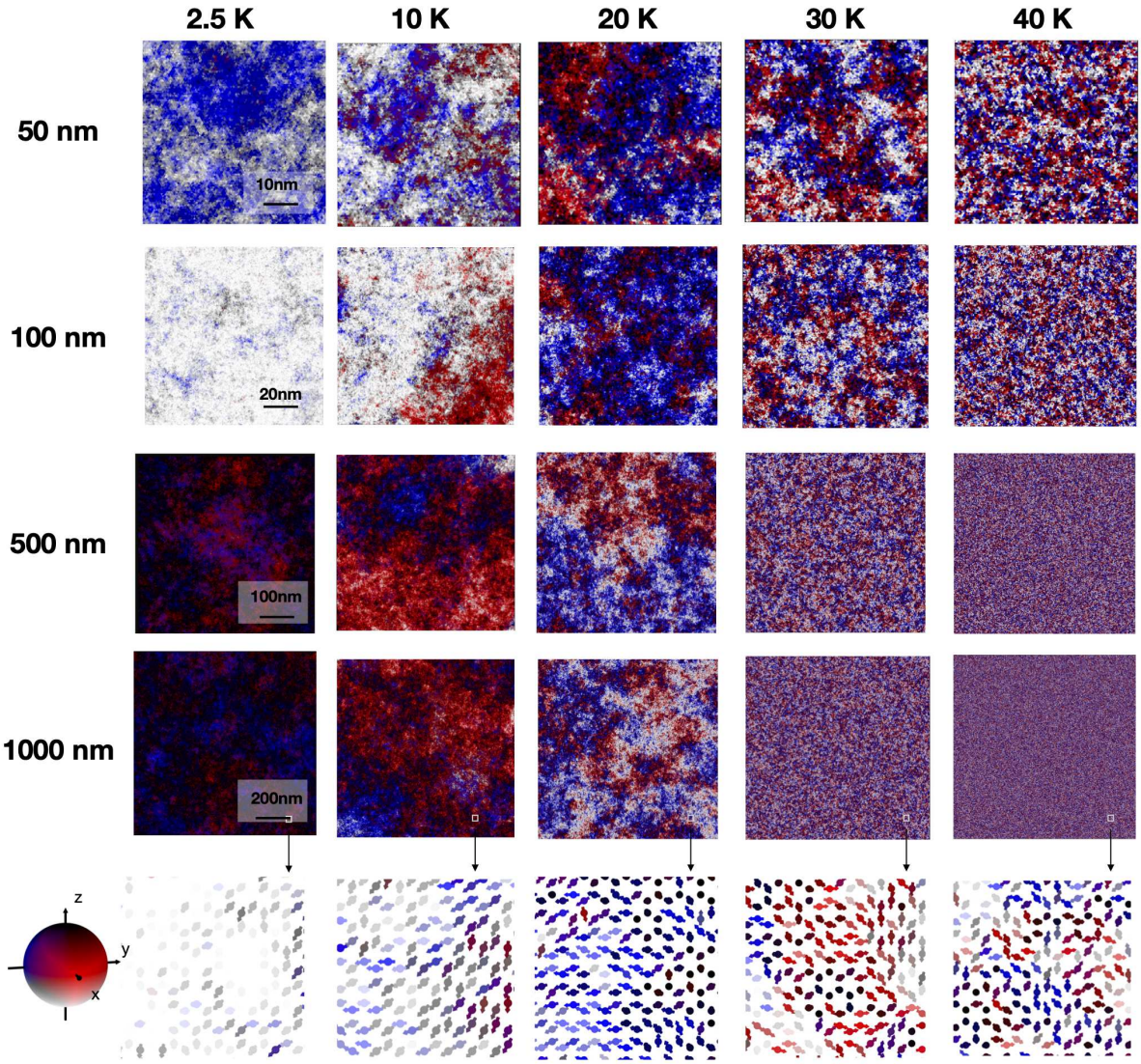

Figure 4: **Temperature-dependent magnetic order.** Visualisations of the magnetic spin configurations for the honeycomb lattice starting from an ordered state as a function of system size (vertical row) and temperature (horizontal row). The spins are projected following the color scale shown in the sphere on the left. The bottom row shows a local view of the spins inside a 5 nm $\times$ 5 nm area at the location outlined by the small boxes in the 1000×1000 nm^2 snapshots.

Supplementary Files

This is a list of supplementary files associated with this preprint. Click to download.

- MerminWagnerSupplementaryInformation.pdf